Assessing the geochemical variability of oil shale in the Attarat Um Ghudran deposit, Jordan

Margus Voolma[a], Alvar Soesoo[a], Väino Puura[b], Sigrid Hade[a] and Hardi Aosaar[c]

[a] Institute of Geology at Tallinn University of Technology, Ehitajate tee 5, 19086 Tallinn, Estonia; margus.voolma@ttu.ee
[b] Department of Geology, Institute of Ecology and Earth Sciences, University of Tartu, Ravila 14A, 50411 Tartu, Estonia
[c] Eesti Energia AS, Lelle 22, 11318 Tallinn, Estonia

Received 4 January 2016, accepted 16 March 2016

Abstract. The Cretaceous to Palaeogene oil shale (OS) of Jordan is predominantly calcareous mudstone with intervals of mostly siliceous minerals, quartz and cristobalite–tridymite. Oil shale is rich in organic sulphur and trace elements. According to preliminary micropalaeontological data, the OS succession of the studied area, the south-central part of the Attarat Um Ghudran (AUG) deposit in central Jordan, is of Maastrichtian age. A representative collection of 392 samples from 9 drill cores reliably characterizes the sequence of the OS seam, on average 70 m thick. The composition of AUG OS varies significantly. The major compounds CaO and SiO_2 range within 3–70 wt% and 10–50 wt%, respectively, and also the contents of organic matter, MgO, P_2O_5, Al_2O_3 and S change. The concentrations of metals (especially Zn, V, Cr, Ni and Mo) change many dozens of times in the cross section. The aim of our statistical analysis was to determine the most significant OS types and their positions in the OS sequence. Two multivariate statistical analysis methods, principal components analysis (PCA) and hierarchical clustering of PCA groups, gave an interpretable result. Four principal components account for 88.6% of data variability. Variation in six main chemical components or groups of components is reflected in parameters of the four principal components. The component PC1 accounts for 47% of the data variance, expressing the highest correlation with organic matter, S, Cr, Cu, Ni, Zn, Mo, and PC2 accounts for 22.82% of the data variability, being strongly correlated with TiO_2, Al_2O_3, Fe_2O_3, SiO_2 and K_2O and negatively correlated with CaO. The next two significant component groups express covariance with CaO and MgO. The applied statistical analysis proves to be a powerful tool for the interpretation of the chemically variable structure of the OS unit when using a representative enough sample collection. In the complex study of the OS unit, variation in the chemical composition is of interest, especially in the context of genetic and mining aspects.

Key words: oil shale, Maastrichtian, mineral matter, geochemical variability, Attarat Um Ghudran deposit, central Jordan.

INTRODUCTION

Jordan is extraordinarily rich in oil shale (OS) resources. Abed & Amireh (1983) have summarized the early (1959–1980) publications on the occurrences of OS in Jordan. At that time, OS was considered as a major future energy resource in Jordan devoid of oil. Subsequent prospecting and exploration campaigns organized by the Government (Hamarneh et al. 2006) cleared the way for developers interested in acquiring concessions in order to initiate the resource exploration and feasibility studies by interested companies. The Estonian–Jordanian company Jordan Oil Shale Energy (JOSE) applied for the concession in the southern part of the Attarat Um Ghudran (AUG) deposit (Fig. 1).

Nevertheless, systematic study of OS chemical composition and its variation in connection with the internal structure of the OS unit was never performed, within the AUG deposit or elsewhere in Jordan. However, recent facies (Powell & Moh'd 2011) and micro-biostratigraphic (Alqudah et al. 2014a, 2014b, 2015) studies enable us to converge to the interpretation of the observed variable geochemical nature of OS accumulation. During 2008–2013, JOSE committed a detailed exploration campaign on its concession area. Analyses of the chemical composition were included in these studies.

Chemical investigation was designed to identify the compositions of and variations in the OS layers and resulted with the definition of subunits – OS layers and barren interlayers (Puura et al. 2016). Certain regularities of average composition and contrast anomalies of macro-component and trace element distribution in the total OS unit and its separate layers were defined. Linking the data on palaeogeography and facies with

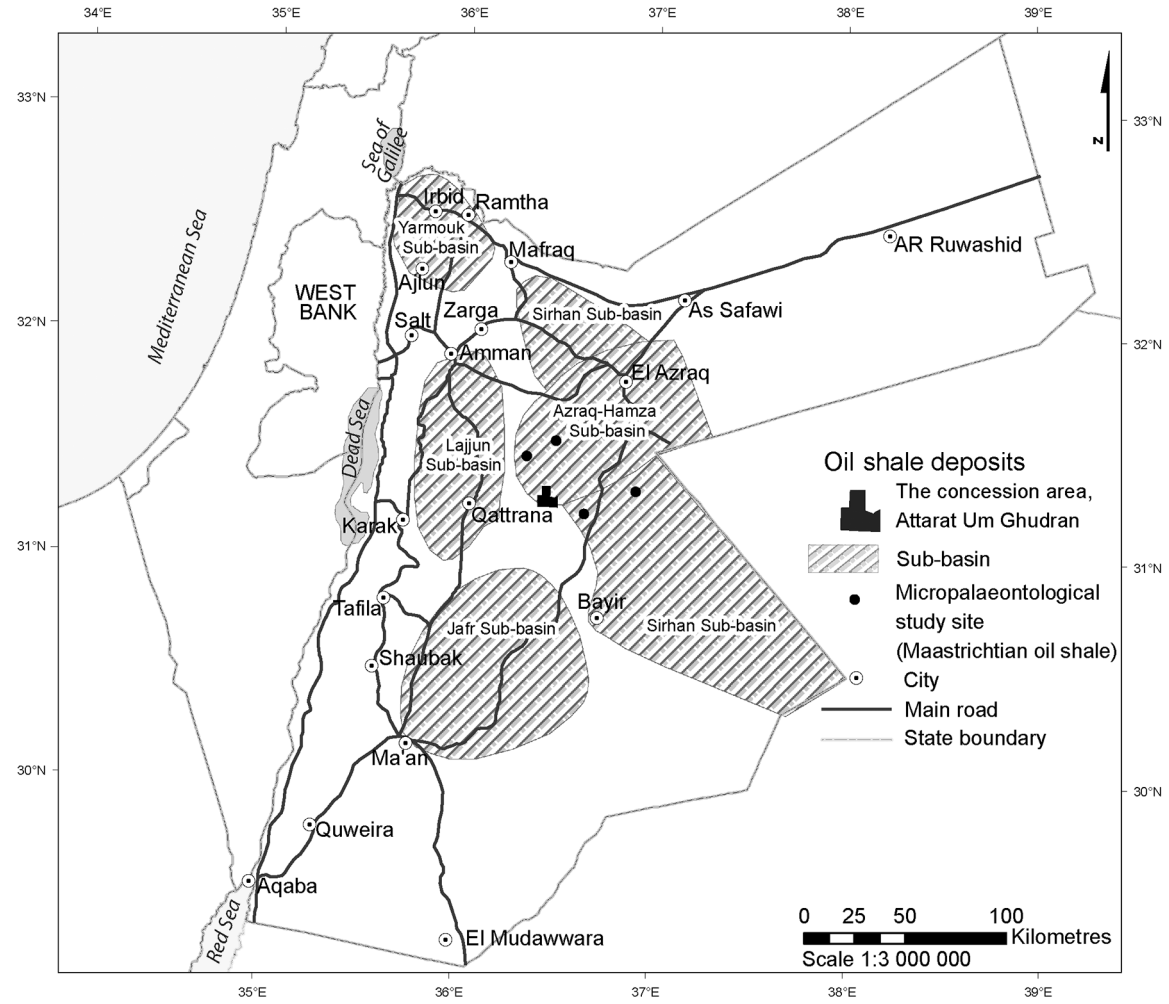

Fig. 1. Approximate location of the JOSE exploration area in the Late Mesozoic to Mid-Palaeogene epicontinental sea platform of Jordan, subjected to the formation of internal shelf basins structured by shallow swells; solid circles – micropalaeontological age studies of drill cores or cuttings (modified from Alqudah et al. 2015).

our data on the variation in chemical composition on a detailed layering scale may deepen the insight into the chemical structure of the OS unit and its separate subunits in the AUG deposit, which actually is now interpreted as having formed in the transition zone from the Azraq-Hamsa Sub-basin to a swell between the latter and the Lajjun Sub-basin. Therefore it is expected that the statistically defined variations in the chemical composition will be useful when considering the development of geological environments of OS accumulation in AUG and conditions of their diagenetic alteration.

As a first step, a systematic geochemical study using different statistical data handling methods is applied. From a list of different methods, results of the principal components analysis are of most interest and presented herein.

The oil shale unit of the JOSE concession area

The AUG deposit, one of many OS deposits of Jordan (Hamarneh et al. 2006; Puura et al. 2016), is located on the Central Jordan desert plateau at altitudes of 700–800 m above sea level, about 100 km southeast of Amman and 40 km east of the village of Qattrana. During 2008–2013, JOSE explored a concession area of about 73 km^2 (Fig. 1). Within the JOSE concession area, the OS unit and the whole OS-bearing Muwaqqar Formation (MCM) is usually flat-lying and only weakly deformed. The total thickness of the MCM locally reaches 150 m, of which the lower part up to almost 100 m is in places composed of OS. According to preliminary micropalaeontological data, the OS succession of the JOSE area is of Maastrichtian age. The non-OS MCM is

exposed in wadi valleys and lower slopes of hills. A hiatus between the MCM and the overlying Umm Riham Chert Limestone Formation corresponds to the Paleocene. The Eocene Riham Chert Limestone Formation, up to 50 m thick, is represented by non-OS chert and marl beds composing tops of jabels (watersheds between the wadi valleys).

The AUG deposit, together with the Wadi Maghara deposit, form a uniform north–southerly elongated OS deposit on a territory of over 1000 km^2 with total resources over 55 billion tons (Hamarneh et al. 2006). The basin and the exploration area have an east-central position among a large number of OS deposits known in Central Jordan (Fig. 1). Detailed lithological and chemical studies conducted in the JOSE concession area suggest that the OS unit consists of lithologically differing OS layers and dolomitic limestone interlayers (Puura et al. 2016). Data on average concentrations of macro- and trace element contents demonstrate significant differences between the layers and variations within the layers. Consequently, the conditions of OS accumulation in the basin have repeatedly changed, which has neither been described nor interpreted so far.

Geological setting of the Attarat Um Ghudran and Wadi Maghara deposits

Geologically, the territory of Jordan is located in the northwest part of the Arabian Plate. Starting in the Palaeozoic, a thick sedimentary cover evolved during several phases (Sharland et al. 2001; Powell & Moh'd 2011). Systematic lithofacies studies of the Cretaceous to Eocene succession in central and southern Jordan (Powell & Moh'd 2011) revealed that (i) the area is characterized by passive continental margin depositional sequences, which pass upwards from alluvial/paralic to carbonate shelf and pelagic ramp settings, and (ii) sedimentation during the Santonian to Maastrichtian was characterized by a hemipelagic chalk–chert–phosphorite lithofacies association, deposited in shallow to moderate water depths on a homoclinal ramp setting, although thicker coeval sequences were deposited in extensional rifts.

Throughout the Early Cretaceous to Eocene, the large temporarily submerged shallow marine clastic and carbonate platform surrounded the continental area of the Arabian Shield in the south and was surrounded by a deep marine clastic and carbonate platform of Neo-Tethys in the northwest (the Mediterranean Neo-Tethys Domain) and northeast (the Eastern Neo-Tethys Domain) (see fig. 1A in Alqudah et al. 2015). Due to upwelling systems, there, the shallow marine deposits contain rich OS and phosphate accumulations (Abed 2013).

A comprehensive and representative study of nanno-fossils from OS sequences of Jordan was committed and OS sequences of Maastrichtian, Paleocene, Early Eocene and Middle Eocene age were identified by Alqudah et al. (2014a, 2014b, 2015). The data revealed that the thickest OS sequences occur in deep sub-basins that developed due to synsedimentary subsidence of the seabed in active fault zones. The accumulation of the OS-bearing and other deposits in the rifting-induced sub-basins and on swells was strongly influenced by climate, tectonic processes and relief of the hinterland. All these factors are supposed to have controlled the influx of terrigenous material (Alqudah et al. 2015). Due to asynchronous subsidence histories of the basins, the location of Maastrichtian, Paleocene and Eocene OS suites in Jordan varies substantially.

Based on reconstructions by Alqudah et al. (2015), the uniform area of the AUG and Wadi Maghara oil shale deposits lies in the transition zone between the deepest zones of the El-Lajjun Sub-basin with Maastrichtian OS (in the west) and the Azraq-Hamza Sub-basin with Maastrichtian–Eocene and locally with over 500 m thick Eocene OS (in the east). The Jafr Sub-basin with Maastrichtian–Eocene OS (locally over 250 m thick) is situated some 100 km to the south. The maximum up to almost 100 m thickness of the Maastrichtian OS unit of the JOSE concession area is less than the deepest parts of the listed sub-basins, but still considerable.

Within the exploration area, the OS unit is of stable internal structure – eight OS layers and three dolomitic limestone interlayers have accumulated uniformly. However, its structure probably changes markedly away from the JOSE concession area. The relatively shallow JOSE sedimentation area is detached by deep basins and swells from both the Arabian-African continent far (over 200 km) in the south and from the Mediterranean Neo-Tethys Domain (palaeo-ocean) in the NE (150 km). Alqudah et al. (2014a, 2015) describe changes in sea-level and land-sea configurations and provide data on synchronous or asynchronous as well as compressional or tensile tectonic stresses causing uplift or subsidence in different fault belt-related deep sub-basins.

MATERIAL AND METHODS

An overview of the chemical composition of Jordan oil shales from different localities has been presented by Abed et al. (2009) and Dyni (2003). In historical studies, however, sampling was sparse and random, and the list of the components analysed was usually incomplete. Unlike previous studies, the present study is based on a representative, systematic sample collection. The samples

are owned by JOSE and only abstract contents of elements can be presented here. Using different analytical techniques (XRF and ICP-MS), the concentrations of more than 40 elements were determined in OS and the surrounding rocks. Geological field and laboratory studies confirmed that primarily the OS layers have accumulated as continuous layers across the whole exploration area. In places, the topmost layers have altered due to weathering, hence the varying thickness of the OS sequence in different drill cores; those samples have been omitted from the data handling and interpretations. For the present detailed geochemical study, 392 samples from nine representative drill cores out of 36, characterizing the full sequence of OS in the JOSE area, were selected. The average thickness of one sample is 1.58 m; the number of samples in a drill core varies from 37 to 55, representing on average 70.1 m of the OS sequence. For the variation and position of lithologically different OS types and thicknesses of individual OS layers along with the chemical composition variation of major elements in the cross section see figure 3 in Puura et al. (2016).

Bisected drill cores were logged and photographed in Jordan. Samples for quality assessment were taken from lithologically uniform intervals with a 0.5–2.0 m step, continuously without any gaps (breaks) between the intervals, coarse-crushed and sent for analyses. The sampling and sample preparation methodology used guarantees a high reliability of (weighted) average compositions of sample intervals, separate OS layers and barren interlayers and the total OS seam.

About 60 g of material was separated from a coarse-crushed sample (< 2 mm) for chemical and mineralogical analysis, using a Humboldt riffle-type sample splitter. The samples were dried in an oven over 24 h at 105 °C. For XRF, XRD and ICP-MS analysis the samples were fine-crushed (pulverized) in a ring mill. Loss on ignition (LOI) was determined from 1 g of pulverized sample material at 500 °C and 920 °C. X-ray fluorescence analysis was conducted at the Institute of Geology at Tallinn University of Technology (IG TUT) with an S4 Pioneer Spectrometer (Bruker AXS GmbH), using an X-ray tube with a rhodium anode, which operated with the power of 3 kW. The samples were measured with a manufacturer's standard as MultiRes modification (pre-calibrated standardless method). The in-house standard ES-2 ('Dictyonema Shale') was used as reference material (Kiipli et al. 2000). The detection limits for trace elements analysed with XRF at the IG TUT are 10 ppm for Ni, Cu, Zn, Ga, Ge, As, Se, Br, Rb, Sr, Y, Zr, Nb, Mo, U, Th, 20 ppm for Sc, V, Cr, Co, Ag, Cd, Sn, Sb, Te, Pb, W, 50 ppm for I, Cs, Ba, La, Ce, Nd and 0.1% for F.

All lithological layers more than 0.5 m thick were sampled separately, however, thin (<50 cm) interbeds seldom observed in the sequences are mixed with material of surrounding thick layers. Therefore certain anomalous varieties of OS or barren rock remain chemically unrecorded. The chemical composition of 1284 samples was analysed. All geochemical data used in this work were acquired during the exploratory programme according to the contract between Enefit/JOSE and the IG TUT. Variation in the chemical composition of 392 samples, forming a regular dataset, from nine representative drill cores (with complete OS sequences) is described by 18 elements whose concentrations constantly exceed the analytical detection limit. The elements and components used in this study are SiO_2, TiO_2, Al_2O_3, Fe_2O_3, MgO, CaO, K_2O, P_2O_5, S, LOI500°C reflecting organic matter (OM), Zn, Ni, Cr, Cu, Mo, V, Zr and Sr. The rest of the analytical dataset (over 600 more samples and over 20 more components in all samples appearing partially in concentrations below the detection level) is used in ongoing geochemical studies and serves as background information herein.

Linking geochemical patterns of a sediment succession with a number of known and unknown geological factors requires a complex multi-step multivariate analysis. As a first step, the statistical analysis is applied in order to define variations and highlight changes in major and trace element compositions that may be linked to certain fluctuations in the course of accumulation of the primary OS sediment and other contemporary and later processes. One of the well-known statistical tools is principal component analysis (PCA), which is the general name for a technique that uses sophisticated underlying mathematical principles to transform a number of possibly correlated variables into a smaller number of variables called principal components. In general terms, PCA uses a vector space transform to reduce the dimensionality of large datasets (like geochemical analyses). Using mathematical projection, the original dataset, which may have involved many variables, can often be interpreted in just a few variables (the principal components). The examination of the reduced dimension dataset will allow the user to spot trends, patterns and outliers in the data, far more easily than would have been possible without performing the PCA.

The dataset for present statistical analyses is composed of 392 data rows as chemical analyses and 18 columns as elements (9 drill cores by 18 elements). Two methods of multivariate analysis were used for data assessment: (i) PCA and (ii) hierarchical clustering of PCA groups. Both analyses were carried out by using software 'R' (package 'FactoMineR') and RExcel. A detailed description, the formulas used and the mechanism of the construction for these parameters are given by Le et al. (2008) and Husson et al. (2010, 2011).

General geochemical characteristics of oil shale in the Attarat Um Ghudran deposit

In addition to small-scale dolomitic limestone layers, two large types of OS can be distinguished in the cross section: (i) mudstone OS that is dark brown to black, almost massive or very finely laminated and (ii) wackestone OS that contains varying amounts of grains (fossil shells and shell debris) and concretions (Puura et al. 2016). According to SEM-EDS observations, grains and concretions in the OS are predominantly calcitic or, in places, carbonate fluorapatite in composition.

In general, according to XRD studies, the mineral composition of OS is limited to calcite, carbonate fluorapatite, quartz (with additional tridymite–cristobalite in certain intervals) and smectite with minor pyrite, sphalerite and barite identified so far (Puura et al. 2016). The variation through the cross section is significant. The content of calcite varies from 8% to 88%, quartz to 51% (cristobalite + tridymite to 47%), and dolomite from below the detection limits (approximately <2%) to 80%, apatite to 40% and clay minerals range to 31%. The corresponding chemical and mineralogical composition is similar to that of the Lajjun deposit, located westwards from the current study area as described by Hufnagel (1984) and Abed et al. (2009).

Despite the dominating carbonate composition of the OS suite, the mineral and chemical composition of the AUG OS seam still varies significantly in cross section (Table 1). Major element composition studies indicate that SiO_2 and CaO range within 3–70 wt% and 10–50 wt%, respectively, and show strong inverse correlation (Fig. 2). The usually low MgO and P_2O_5 content rises randomly up to 16 wt%. The Al_2O_3 and S concentrations are locally up to 7 wt% and 6 wt%, respectively. The OM content in the deposit varies from 4 wt% to 38 wt%. A significant variation occurs also in trace metal contents, for Zn and V ranging within 100–2784 ppm and 78–2040 ppm. Ni, Cr and Mo show concentrations from a few tens of ppm to 488, 626 and 614 ppm, respectively.

Geochemical variation in major and trace elements significantly depends on the layered structure of the OS unit (Table 1). Apart from lithological OS types, there are geochemical distinctions separating different OS layers, indexed A to E3. Unlike the rest of the layers, certain OS layers show distinct enrichment in some elements, for example, kerogen- and trace metal-rich layer E2 (Fig. 2, Zn vs Ni plot), SiO_2-rich layer D, CaO-rich and SiO_2-poor layers E3 and E1 (Fig. 2, SiO_2 vs CaO plot) and P_2O_5-rich layer A (Fig. 2, P_2O_5 vs CaO plot). The dolomitic limestone

Table 1. Mean, minimum and maximum concentrations of chemical elements in 392 samples and average thickness of 398 samples from nine drill cores; and average thickness and concentrations by different oil shale and barren rock layers (A–E3) distinguished in the concession area, Attarat Um Ghudran deposit, Jordan. Organic matter (OM) reflected by LOI500°C. Major elements in wt%, trace elements in ppm. (The chemical composition of dolomitic limestone layers A/B, B/C and D/E was not analysed in two drill cores)

	Total data			Average by distinguished layers										
	Mean	Min	Max	A	A/B	B1	B2	B/C	C	D	D/E	E1	E2	E3
Number of samples	392 (398)			66	7 (9)	38	84	7 (9)	44	28	7 (9)	45	22	44
Thickness (m)	1.59	0.50	2.00	1.51	0.78	1.70	1.73	0.55	1.68	1.54	1.15	1.63	1.57	1.69
SiO_2	18.90	2.59	71.70	29.23	5.97	19.75	19.88	8.79	22.21	40.13	9.21	8.84	7.59	5.13
TiO_2	0.08	0.02	0.29	0.05	0.04	0.05	0.09	0.05	0.10	0.20	0.07	0.08	0.06	0.05
Al_2O_3	2.02	0.38	6.97	1.28	1.15	1.18	2.29	1.67	2.56	4.84	1.99	2.20	1.64	1.20
Fe_2O_3	0.63	0.21	1.77	0.49	0.37	0.46	0.65	0.43	0.76	1.27	0.49	0.65	0.66	0.44
MgO	1.37	0.22	15.50	1.13	11.99	0.46	0.84	9.88	0.77	1.28	12.29	0.63	0.54	0.59
CaO	33.91	10.79	49.26	30.34	34.73	36.20	32.98	33.13	30.82	18.87	31.97	41.48	34.75	43.84
K_2O	0.25	0.06	0.62	0.22	0.11	0.18	0.34	0.21	0.35	0.41	0.13	0.22	0.19	0.12
P_2O_5	2.82	0.47	16.58	5.03	1.38	3.85	3.01	1.63	3.20	1.80	0.72	1.91	0.97	1.12
S	2.68	0.54	6.22	2.65	0.80	2.66	2.82	1.18	2.98	2.81	0.72	2.24	4.73	2.37
OM	16.02	4.13	38.28	13.17	6.13	14.85	17.30	8.03	18.65	16.37	5.77	14.53	29.13	15.43
Zn	862	100	2784	876	176	764	769	288	946	856	149	657	2035	954
Ni	173	28	488	148	43	158	167	66	193	163	35	151	378	203
Cr	292	83	626	230	108	241	312	152	331	328	105	284	488	320
Cu	60	<10	131	61	16	62	61	25	65	53	12	53	106	60
Mo	143	12	614	136	17	96	133	36	170	180	19	103	348	157
V	436	78	2040	508	113	341	292	114	388	427	98	347	1395	508
Zr	38	<10	85	28	16	33	43	21	43	48	29	39	44	36
Sr	680	229	1855	585	375	729	697	432	710	568	565	759	769	770

interlayers show compositionally extreme values for certain elements, especially MgO (layers A/B, B/C, D/E) (Fig. 2, MgO vs CaO plot). The OS layers (A–E3) and barren interlayers can be followed at least across the JOSE study area. A selection of X–Y correlation graphs (Fig. 2) illustrates cases of strong positive, negative and less significant correlation relationships of main and trace elements, varying also by the layers. However, the internal chemical structure and the compositional changeability within the layers are difficult to assess visually or by using simple correlation methods. This is the reason why statistical multivariate methods have been applied to transform a number of possibly correlated variables (chemical elements) into a smaller number of variables, which can be later interpreted through geological processes and elemental composition.

DISCUSSION

Traditionally, the oil shales of the Muwaqqar Chalk-Marl Formation of Jordan are described as predominantly uniform kerogen-bearing calcareous rocks, most frequently named just as chalk and marl (Abed 2013; Alqudah et al. 2014a, 2015). Systematic and regular sampling and analyses of the full OS succession in Central Jordan have changed the image. The JOSE exploration process revealed the stable internal layered structure of the OS unit caused by compositional variations (Puura et al. 2016). Together with general lithological data, mineral composition and gamma-log survey, the specific chemical compositions and geochemical contrasts of layers served for the complex definition of OS layers and barren interlayers in the OS unit of the JOSE exploration area. The dominating thick OS suite is separated into subunits by thin but continuous barren interlayers of dolomitized limestones, and other marker surfaces. Besides the principal layered structure of the OS unit, regular differences between mineral and average chemical compositions of layers were established, as presented in Table 1.

As the first step in assessing the geochemical variability, statistical analysis is applied in order to define major and trace element variations and contrast main changes in the sedimentary sequence of OS and barren rock. The definition of distinct geochemical patterns among and also inside the distinguished layers is an additional result of the study. Further on, the integration of statistical and geological results will help to study trends and changes in the accumulation of original sediments – OS layers, barren rock interlayers, and their internal variability.

Principal component analysis for distinguishing the geochemical characteristics and clustering of samples

Nine drill cores across the AUG OS deposit, each represented by approximately 45 samples described by 18 variables (chemical elements), were chosen for PCA. The aim of the statistical analysis is to determine significant types of different OS and barren rock and their position in the overall sequence of the OS unit in combination with geochemical patterns.

Principal component analysis and the hierarchical clustering of PCA groups are used for geochemical data assessment. Eigenvalue, derived from PCA, is a measure of quality of data representation and shows the relative importance of the components. In the present dataset, four principal components are significant, as each of those accounts for over 10% of variability. The first principal component (PC) accounts for 47.11% of data variability, the second component for 22.82%, while four components together account for nearly 90% of data variability (70% by the first two components; Fig. 3). In order to visualize interrelationships between PC and chemical elements (Table 2), the planes constructed by pairs of principal components PC1 to PC4 (Fig. 4) are presented. Plots of single samples (grouped into clusters) on the planes PC1–PC2 and PC1–PC3 demonstrate association between clusters and principal components (Fig. 5). When interpreting the geochemical data and elemental variation parameters, it is important to consider the main carriers of major and trace elements: calcite as the carrier of CaO; dolomite as the carrier of CaO and MgO; quartz (and modifications) – SiO_2; clay minerals – Al_2O_3, SiO_2, K_2O, TiO_2; carbonate-fluorapatite – P_2O_5, CaO; organic matter – expressed as LOI500°C (includes part of sulphur and carries Zn and many other trace metals).

Relying upon the described methodology, the interpretation of significant principal components is given below.

PC1 – The first PC describes 47% of the data variance. It is strongly correlated with many variables (Table 2), with the highest correlation with S and OM (LOI500°C), and also Cr, Cu, Ni, Zn and Mo. Very strong correlation between OM, S, and trace metals suggests that these elements vary together. This component can be interpreted as a measure of sulphur- and trace-element-carrying OM versus carbonate-silicate mineral matter (calcite, dolomite, silica) content.

PC2 – The second PC accounts for 22.82% of the data variability. It is strongly correlated with TiO_2, Al_2O_3, Fe_2O_3, SiO_2 and K_2O. Strong negative correlation occurs with CaO (Table 2). The component can be

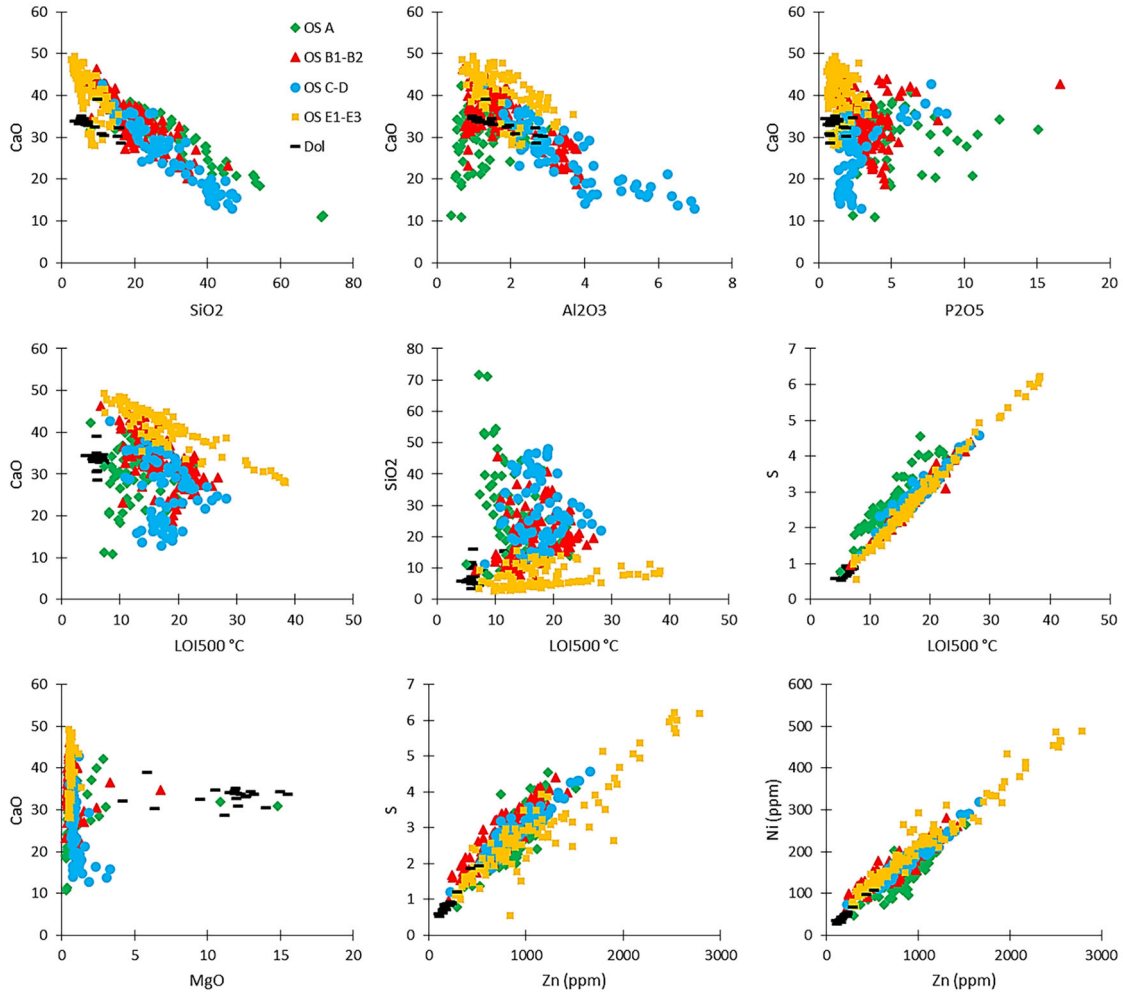

Fig. 2. A selection of X–Y plots between 9 elements, selected out of the studied 18 using analytical data on single samples. The plots demonstrate the best examples of variable nature of correlations between certain different components of the oil shale (OS) unit in total: (i) strong negative (CaO vs SiO_2) or moderate negative (CaO vs Al_2O_3) or scattered (CaO vs P_2O_5) correlation between the main mineral components of OS, (ii) scattered (diffuse) correlation between the CaO and SiO_2 contents and LOI500°C, the latter reflecting the content of organic matter, (iii) strong positive correlation between LOI500°C and S, and further on between S and Zn, and Zn and Ni. The plots reflect also distinct geochemical differences between certain layers and the rest of samples, e.g. layers C and D on the CaO vs Al_2O_3 plot and layers E1–E3 on many plots. The MgO vs CaO plot expresses the presence of elevated MgO contents only in barren dolomitic limestone layers.

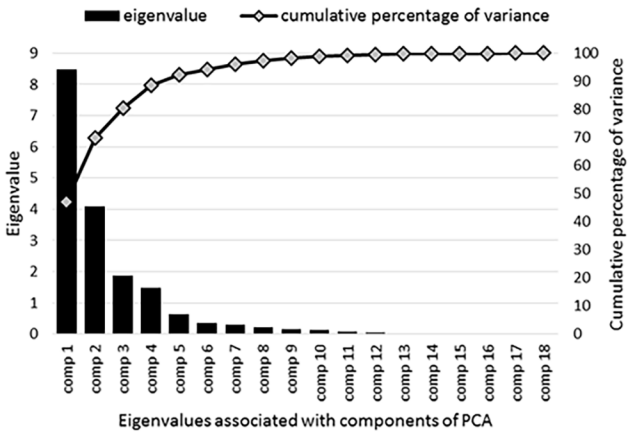

Fig. 3. Bar plot of the eigenvalues showing the number of components significant for interpretation. In the present dataset, the first four components account for 88.66% of variability.

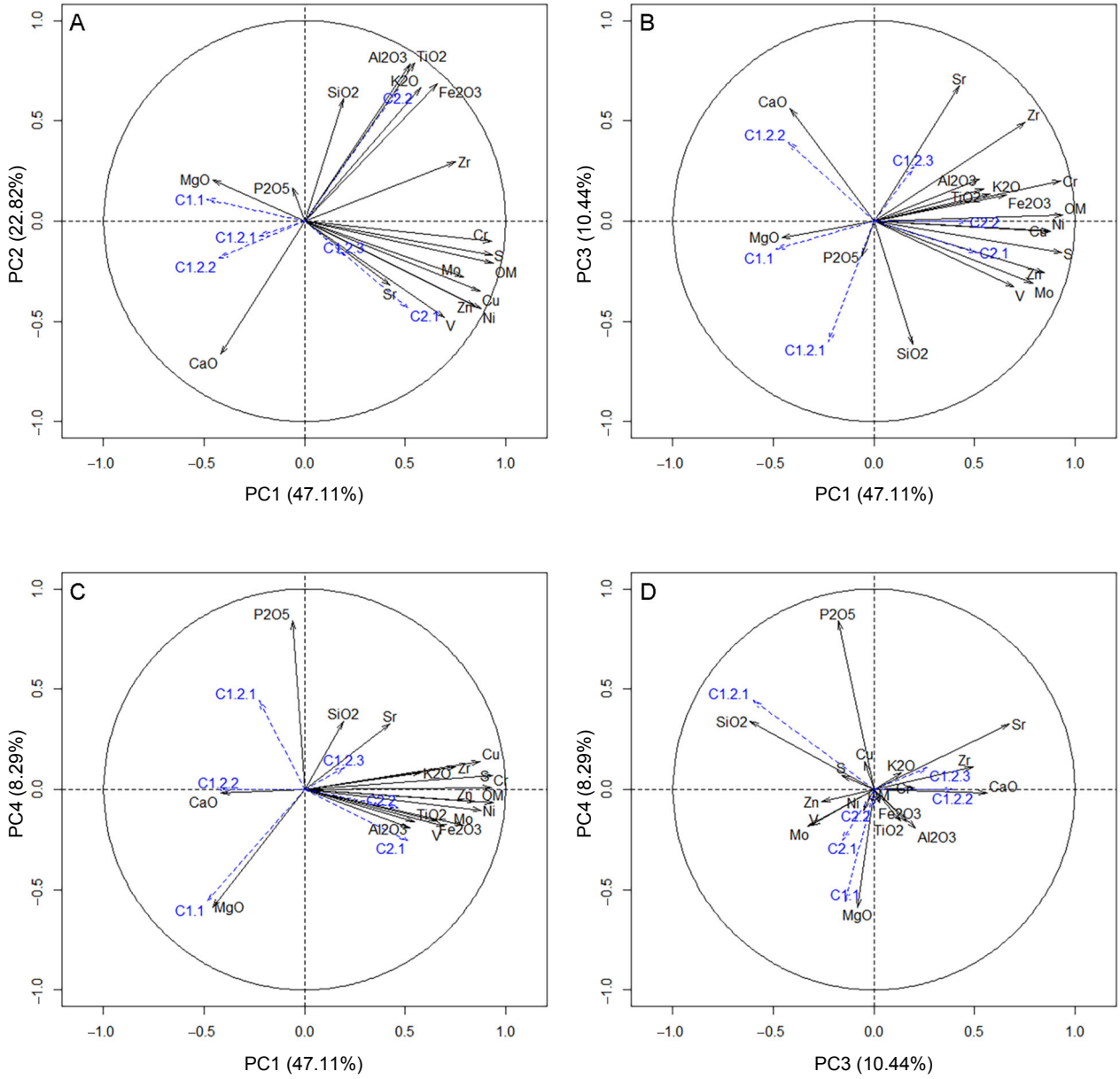

Fig. 4. Graphs of the analysed major and trace elements on the planes constructed by principal components. The distance between the chemical component projected onto a plane and the correlation circle with radius 1 demonstrates the correlation of the variable and principal components (Table 2). The distance from an axis shows the quality of how well the element is projected onto a corresponding plane. The proximity of variables on the plane means also strong association between individual elements (for example OM and S on planes A, B and C; see also Fig. 2 LOI500°C vs S plot). Clusters (C1.1 to C2.2) are presented to demonstrate the association between chemical components and principal components (see text for the explanations). On a main plane (explains 69% of variability) constructed by principal components PC1 and PC2, OM (LOI500°C), S, Cr, Mo, Cu, Zn and V are positively correlated to PC1, while MgO and CaO are negatively correlated to PC1. It means that samples with a high concentration of MgO have a low content of OM (LOI500°C), S, Cr, Mo, Cu, Zn and V, and vice versa. Strong positive correlation is between TiO_2, Al_2O_3, Fe_2O_3, SiO_2, K_2O and PC2, while CaO is negatively correlated to PC2. Thus the samples with a high CaO content have low TiO_2, Al_2O_3, Fe_2O_3, SiO_2 and K_2O contents, and vice versa.

interpreted as 'silicates' (clay, silica in mud ground mass and chert) versus 'calcic' components in the OS.

PC3 – Sr, SiO_2 and CaO contribute the most to the formation of the third component that describes 10.44% of the data variance. The third PC has a positive correlation with Sr and CaO, while the correlation with SiO_2 is also strong but negative (Table 2). This component can be interpreted as a measure of biogenic calcite (calcite mud, foraminifera shells, carbonate skeletal debris) versus silica amounts in OS.

PC4 – The fourth component accounts for 8.29% of data variability. Significant positive correlation with P_2O_5 contents, weaker negative correlation with MgO and lack or low correlations with all other elements suggest that PC4 describes processes of phosphorus enrichment, including apatite skeleton debris in OS.

Principal component analysis proves that considerable variation exists in chemical composition among the studied OS and barren rock samples. Based on Figs 4 and 5, it can be concluded that the OS sequence contains OS subtypes with very high OM and metal contents, and dolomite samples with a very low content of metals. There are samples with a high calcite content and a low quartz content and vice versa, and samples with a considerable amount of OM accompanied by a variable mixture of calcareous and siliceous mineral matrix. In addition, samples with a high apatite content are also found in the OS succession.

Table 2. Correlation between principal components and variables. The first two variables contributing the most to the construction of the corresponding component are in bold. Variables on the plane induced by different components are presented also in Fig. 4

	PC1	PC2	PC3	PC4
SiO_2	0.19	0.61	**−0.62**	0.34
TiO_2	0.55	**0.79**	0.16	−0.16
Al_2O_3	0.52	**0.78**	0.21	−0.19
Fe_2O_3	0.66	0.69	0.13	−0.16
MgO	−0.46	0.21	−0.08	**−0.59**
CaO	−0.42	−0.67	0.56	−0.02
K_2O	0.58	0.66	0.14	0.08
P_2O_5	−0.06	0.17	−0.18	**0.84**
S	**0.93**	−0.17	−0.16	0.07
OM	**0.94**	−0.21	0.03	−0.06
Zn	0.85	−0.43	−0.26	−0.06
Ni	0.88	−0.44	−0.05	−0.10
Cr	0.93	−0.10	0.20	0.01
Cu	0.87	−0.35	−0.05	0.14
Mo	0.79	−0.28	−0.31	−0.18
V	0.70	−0.48	−0.33	−0.18
Zr	0.75	0.30	0.49	0.11
Sr	0.42	−0.32	**0.67**	0.33

The current dataset consists of samples from nine drill cores covering the lateral and vertical extent of the OS deposit. Approximately 45 samples from each core represent an on average 70 m thick vertical cross section of the 72 km^2 deposit area. As recorded from the chemical composition of the OS sequence, the deposition of 70 m of OS took place in a considerable time period (by indirect assessment, a few millions of years), during which stable and variable conditions of accumulation alternated. These variations become visible by the help of hierarchical clustering of samples using PCA.

The hierarchical classification of 392 samples is presented in Fig. 6. Two distinct groups are separated, C1 and C2, which are further subclustered into C1.1, C1.2, and C2.1, C2.2, respectively. Cluster C1.2 is additionally subdivided into three subclusters: C.1.2.1, C1.2.2 and C1.2.3. The principal components describing different clusters are plotted in Fig. 5, and the relation of elements to clusters on planes constructed by components is visualized in Fig. 4.

The geochemical pattern is plotted using the average of the element in the cluster, normalized to the average of the element concentration in the whole dataset. It enables us to highlight the range of variation of different elements (including those non-significant for defining a certain cluster) in the limits of a geochemical group and between the groups (Fig. 7).

Positioning of clusters in oil shale sequences reflecting changes during oil shale accumulation

The properties of the studied OS subunits (Table 1) are shortly summarized as follows: **OS layer A** is described as phosphate-bearing OS; **OS layer B1** is terminated by OS layer B2 with the disappearance of phosphate concretions in OS; **OS layer B2** is currently separated as calcareous-siliceous OS; **OS layer C** is currently defined as calcareous-siliceous OS; **OS layer D** is described as SiO_2-rich; **OS layer E1** is calcareous; **OS layer E2** is OM-rich and has a high content of metals; **OS layer E3** is calcareous. Three dolomitic limestone interlayers (A/B, B/C, D/E – in the geochemical study altogether indexed as Dol) subdivide the OS seam into four parts: A, B1+B2, C+D and E1+E2+E3.

The positions of individual samples in OS cross sections are plotted in Fig. 8, using the cluster colour legend from Fig. 7 and others. The cluster analysis proves that samples are clustered along the lateral extent of OS layers referring (i) to the persistence of the composition of the layers in the horizontal direction over the exploration area and (ii) to the layering-related alternation of OS chemical types from the bottom to the

top of the unit. Consequently, the results suggest that distinct laterally uniform conditions of the accumulation of OS layers and barren rock interlayers principally (with minor local variations, however) governed the formation of each layer over the whole exploration field. In the vertical succession, uniform variations in the composition of layers and their subunits reflect respective alternation and also trends of sedimentation conditions. Visualizing the distribution of sample groups (corresponding to different clusters) using the colour-coded legend enables us to observe the structure of the OS unit in more different aspects: (i) variability of the unit in general, (ii) co-existence of certain sample groups, (iii) specific assemblages of chemical groups in different layers, (iv) specific composition of the barren interlayers, etc.

The distribution of cluster groups of samples (Fig. 8) expresses also the chemical variability of the OS unit and its separate layers in aspects of the appearance of certain specifically characteristic patterns. Specific characteristics of the sample groups (clusters), presented below, highlight the individual elements or group of elements with high or low levels.

C1.1 – Samples in this group are described by elements (MgO) having low values on a plane constructed by PC1 vs PC4 (Figs 4C, 5). The chemical pattern presented in Fig. 7 shows the MgO concentration several times higher in this group, while other elements are below average. The group is present in only barren dolomitic interbeds A/B, B/C and C/D.

C1.2.1 – The samples in this group are described by elements (P_2O_5, SiO_2) having high values on axis PC4 and low values on axis PC3 on a plane constructed by principal components (Figs 4D, 5). This group is characterized by above-average P_2O_5, together with SiO_2 content (Fig. 7) due to the high apatite (and quartz-chert) contents, while OM, trace metals and clay content are suppressed. The samples of C1.2.1 occur from the footwall and dominate in the OS layers A and B1 (Fig. 8). Minor alternation with other OS types decreases upwards.

C1.2.2 – This group is defined by high values of CaO on axis PC3 and low values on axis PC1 (Figs 4B, 5). The chemical pattern shows the slightly above-average contents of CaO and Sr and the below-average contents of all other elements. These samples are likely representing wackestone-type OS intervals. In the deposit this type of OS appears in 3–4 intervals alternating with other types of OS in layers B1 and B2, and becomes more dominating in the upper part of the OS sequence (Fig. 8).

C1.2.3 – The samples of this group are described by elements having high values on a plane constructed by PC1 vs PC3 (Figs 4B, 5). With slight 'negative SiO_2 anomaly' the chemical pattern of these samples represents the average composition of other types of OS (Fig. 7). This type of OS is present in several OS layers, forming one interval in OS layer B2, major part of layer C, and several continuous intervals in E1 and E3 (Fig. 8).

C2.1 – The samples of this group are described by OM carrying S and trace metals having high values on axis PC1 and low values on axis PC2 (Figs 4A, 5). The differentiating feature of this cluster is OM nearly two times higher and a very high content of trace metals (Fig. 7). These samples form a distinct interval, layer E2, which separates otherwise similar OS layers E1 and E3 (Fig. 8).

C2.2 – The samples of this group are described by elements (TiO_2, Al_2O_3, K_2O, Fe_2O_3) having high values on the plane constructed by PC1 vs PC2 (Figs 4A, 5). The distinctive feature of these samples is the above-average content of Al_2O_3, TiO_2, Fe_2O_3, K_2O and SiO_2 (Fig. 7). In the cross section these samples form a distinct interval in the middle part of the OS unit corresponding to OS layer D; however, three continuous minor intervals also occur at lower levels (Fig. 8).

CONCLUSION

A representative collection of gapless core samples reliably characterizes the chemical composition of the full OS sequence and, within it, of the eight separate OS layers and three dolomitic interlayers forming the OS unit in a limited area of the AUG deposit. The results of PCA and hierarchical clustering of the sample collection provide considerable information about the geochemical pattern – regularities in the distribution of sample clusters within and between the different OS layers. The variation in the chemical composition of the OS unit is basically expressed and visualized with six specific geochemical groups (clusters) of samples, whose spatial distribution allows summarizing the main changes in the composition and shapes of the general chemical patterns of the deposit. The study reveals that significant general trends and fluctuations in the entire OS unit as well as differences in the chemical composition of the individual OS layers occur namely in accordance with the layered structure and have most likely been established by considerable changes in sedimentation conditions. Minor variations as well as specific geochemical stability intervals occur in the internal structure of layers.

The inconstant composition of the OS unit has resulted from different intensity of the accumulation of chemical components that are almost independent

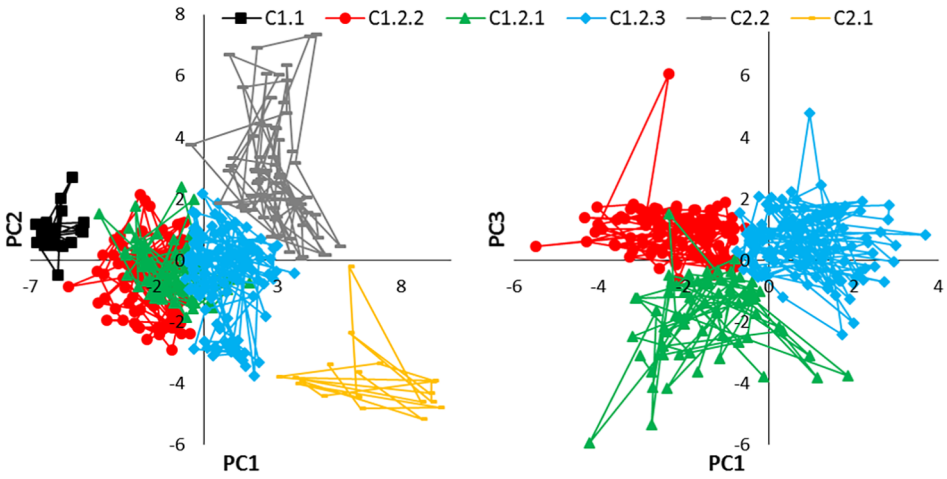

Fig. 5. On principal components planes constructed by PC1–PC2 and PC1–PC3 (and others not presented here), the cloud of the analysed samples grouped into clusters (C1.1, C1.2.1, etc.) demonstrates the correlation between samples and principal components. Note the different positioning of clusters on different planes, showing which component (and elements forming the corresponding component) best describe the samples in the cluster. On the plane PC1 (S, OM, trace metals) – PC2 ('clay components') clusters C1.2.1 (P_2O_5 with SiO_2, typical for the layers A and B1), C1.2.2 (Sr with CaO) and C1.2.3 (nearly corresponding to average oil shale) partially overlap, whereas on the plane PC1–PC3 (Sr and CaO with SiO_2) these clusters are located separately.

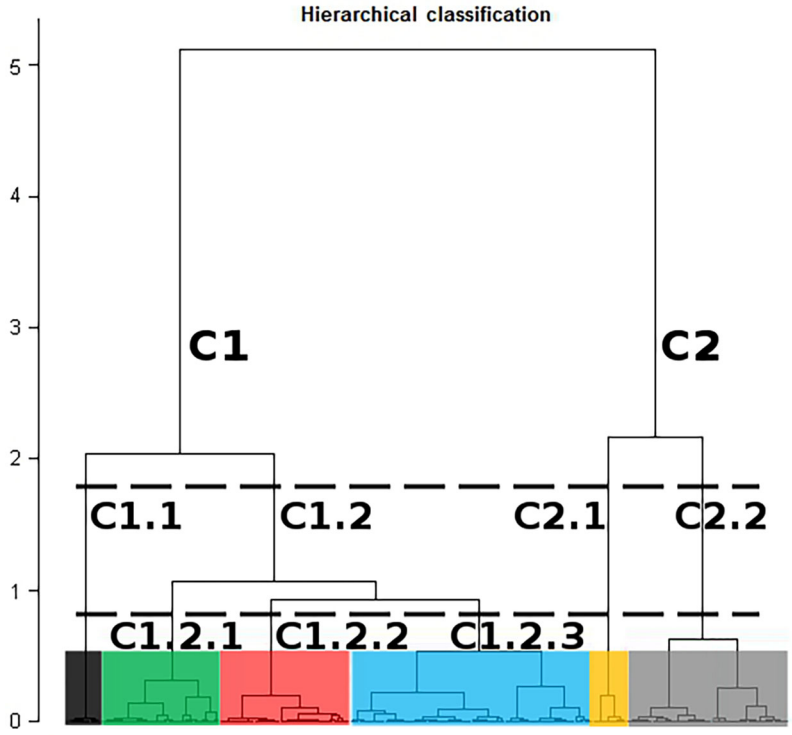

Fig. 6. Hierarchical classification dendrogram. The distance of linkage between samples/clusters is a measure of similarity of individual samples within the cluster or between clusters. The most distant linkage bonds two groups of samples that are further subdivided and samples can be described by a distinguishing component: C1.1 – dolomite (MgO); C1.2.1 – apatite (P_2O_5); C1.2.2 – calcite (CaO); C1.2.3 – 'average oil shale'; C2.1 – organic matter (OM, S, trace metals); C2.2 – silicate (clay-related elements). For the full pattern of 18 elements see Fig. 7. Note that the diagram reflects the number of samples and also the number of varieties in the clusters that are described in the text.

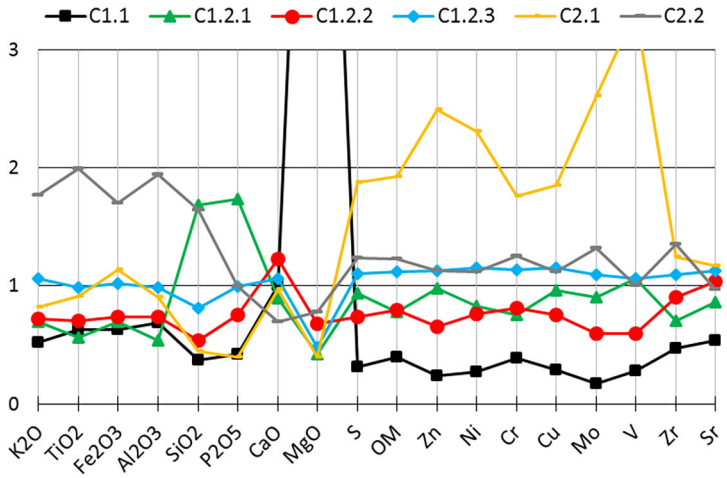

Fig. 7. Geochemical 'patterns' of different clusters showing specific elements that have elevated or low concentrations, thus defining the cluster's geochemical properties: very high MgO defining C1.1 and representing dolomite samples; peak of P_2O_5 (SiO_2) distinguishing apatite-rich samples of the C1.2.1 group; peak of CaO (Sr) with a below the average and flat pattern of other elements representing wackestone oil shale samples of C1.2.2; C1.2.3 being characterized by a flat pattern and close to the average composition; samples of C2.1 distinguished by elevated OM carrying S and trace metals; C2.2 groups samples with above the average content of elements related to silicates.

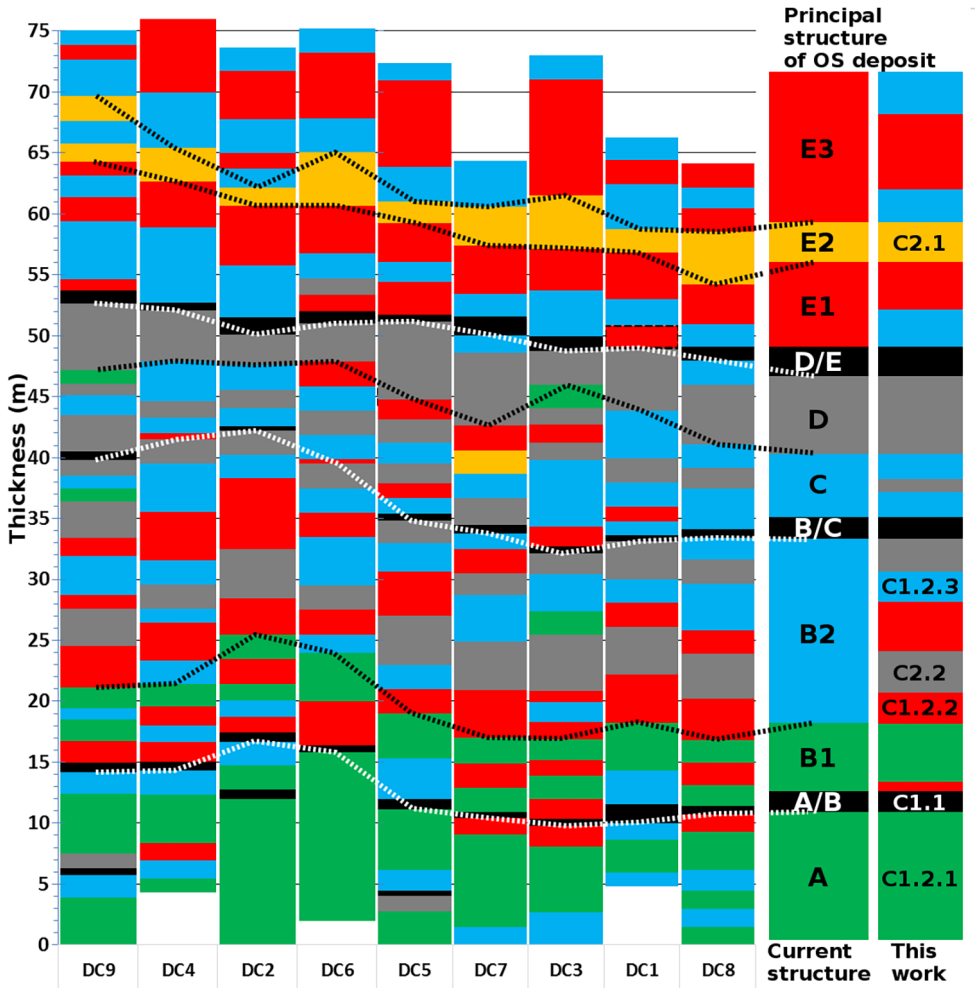

Fig. 8. The position of samples belonging to different clusters in nine oil shale sequences (wells DC1–DC9) revealing the complex structure of the deposit. For better reading three cross sections are uplifted and dashed lines are indicating the base of currently separated oil shale and barren dolomitic limestone layers. For comparison a simplified column of the current structure (NB! layer thicknesses are approximate) with corresponding chemical properties indicated by colours is plotted aside the summarized column of nine cross sections, illustrating the alternation of chemically different types of oil shale/dolomite samples in the sequence.

of each other: (i) CaO of calcite; (ii) SiO_2 of quartz (cristobalite–tridymite); (iii) Al_2O_3 and related elements of clay minerals; (iv) P_2O_5 of apatite and (v) OM carrying S and trace metals (Zn, Mo, Cr, etc.). Exceptional elevated concentrations of MgO in barren carbonate interlayers are likely due to diagenetic processes but derived from specific limestones deposited without load of clay components, apatite and OM carrying sulphur and trace metals.

Principal component analysis integrated with cluster analysis proved to be a powerful tool for the interpretation of the chemically variable structure of the OS unit when using a representative enough sample collection. The integration of chemical data and results of their statistical processing with lithological, mineralogical, palaeontological, petrophysical and other datasets potentially serves for the further interpretation of the origin of OS and barren interlayers. The data are useful also for the development of OS utilization technologies having in mind the variability of their composition.

Huge amounts of OS have accumulated in the Late Cretaceous epicontinental sea 'carbonate shelf' basins of Jordan and neighbouring territories. In these basins, oil shales and leaner kerogen-bearing rocks have similar OM of marinite type and similar predominantly calcareous mineral matter. Surprisingly, the presence of barren rock layers is strongly suppressed. Variations in compositions and respective changes in accumulation conditions expressed in OS profiles of different sub-basins and OS units of different age (from Early Maastrichtian to Early Eocene) are poorly studied so far. Sources of accumulated marine mineral matter in the epicontinental shallow marine maze of pools and swells also remain poorly known. The results of the geochemical studies of the JOSE exploration area within the Attarat Um Ghudran deposit show that integrated geochemical investigations together with nannofossil stratigraphic studies are probably the most promising tool for the comparative research into OS profiles of different sub-basins and of different age units in the region. The integration of mineralogical and more detailed geochemical studies (including the use of components not treated here) could contribute to resolving unanswered questions.

Acknowledgements. We thank companies Eesti Energia AS and JOSE for providing the geological material and permission to use the geochemical data in this work. We are grateful to J. Mutterlose and the anonymous referee whose remarks and comments helped to improve the manuscript.

REFERENCES

Abed, A. M. 2013. The eastern Mediterranean phosphorite giants: an interplay between tectonics and upwelling. *GeoArabia*, **18**, 67–94.

Abed, A. M. & Amireh, B. S. 1983. Petrography and geochemistry of some Jordanian oil shales from North Jordan. *Petroleum Geology*, **5**, 261–274.

Abed, A. M., Arouri, K., Amireh, B. S. & Al-Hawari, Z. 2009. Characterization and genesis of some Jordanian oil shales. *Dirasat: Pure Sciences*, **36**, 7–17.

Alqudah, M., Ali Hussein, M., Van den Boorn, S., Podlaha, O. G. & Mutterlose, J. 2014a. Calcareous nannofossils biostratigraphy of oil shales from Jordan. *GeoArabia*, **19**, 117–140.

Alqudah, M., Ali Hussein, M., Van den Boorn, S., Giraldo, V. M., Kolonic, S., Podlaha, O. G. & Mutterlose, J. 2014b. Eocene oil shales from Jordan – paleoenvironmental implications from reworked microfossils. *Marine and Petroleum Geology*, **52**, 93–106.

Alqudah, M., Ali Hussein, M., Van den Boorn, S., Podlaha, O. G. & Mutterlose, J. 2015. Biostratigraphy and depositional setting of Maastrichtian–Eocene oil shales from Jordan. *Marine and Petroleum Geology*, **60**, 87–104.

Dyni, R. J. 2003. Geology and resources of some world oil-shale deposits. *Oil Shale*, **20**, 193–252.

Hamarneh, Y., Alali, J. & Sawaged, S. 2006. *Oil Shale Resources Development in Jordan*. Natural Resources Authority of Jordan, Amman (updated report), 98 pp.

Hufnagel, H. 1984. Die Ölschiefer Jordaniens. *Geologisches Jahrbuch*, Reihe A, Heft 75, 295–312.

Husson, F., Josse, J. & Pages, J. 2010. *Principal Component Methods–Hierarchical Clustering–Partitional Clustering: Why Would We Need to Choose for Visualizing Data?* Technical Report–Agrocampus Ouest, Applied Mathematics Department, 17 pp.

Husson, F., Le, S. & Pages, J. 2011. *Exploratory Multivariate Analysis by Example Using R*. 1st ed. Chapman & Hall/CRC, London, 228 pp.

Kiipli, T., Batchelor, R. A., Bernal, J. P., Cowing, Ch., Hagel-Brunnstrom, M., Ingham, M. N., Johnson, D., Kivisilla, J., Knaack, Ch., Kump, P., Lozano, R., Michiels, D., Orlova, K., Pirrus, E., Rousseau, R. M., Ruzicka, J., Sandstrom, H. & Willis, J. P. 2000. Seven sedimentary rock reference samples from Estonia. *Oil Shale*, **17**, 215–223.

Le, S., Josse, J. & Husson, F. 2008. FactoMineR: An R Package for Multivariate Analysis. *Journal of Statistical Software*, **25**(1), 1–18.

Powell, H. J. & Moh'd, K. B. 2011. Evolution of Cretaceous to Eocene alluvial and carbonate platform sequences in central and south Jordan. *GeoArabia*, **16**, 29–82.

Puura, V., Soesoo, A., Voolma, M., Hade, S. & Aosaar, H. 2016. Chemical composition of the mineral matter of the Attarat Um Ghudran oil shale, Central Jordan. *Oil Shale*, **33**, 18–30.

Sharland, R. P., Archer, R., Casey, M. D., Davies, B. R., Hall, H. S., Heward, P. A., Horbury, D. A. & Simmons, D. M. 2001. *Arabian Plate Sequence Stratigraphy*. *GeoArabia* Special Publication 2: Gulf PetroLink, Bahrain, 371 pp.

Jordaania Attarat Um Ghudrani maardla põlevkivikihtide geokeemilise muutlikkuse hinnang

Margus Voolma, Alvar Soesoo, Väino Puura, Sigrid Hade ja Hardi Aosaar

Jordaania Kriidi ja Paleogeeni vanusega põlevkivid on valdavalt lubjarikkad mudakivid, mõningate ränirikaste intervallidega, kus domineerivateks mineraalideks on kvarts ning kristobaliit-tridümiit. Esmaste mikropaleontoloogiliste andmete põhjal on käesolevas töös uuritud põlevkivid Maastrichti vanusega. Kesk-Jordaanias paikneva Attarat Um Ghudrani maardla põlevkivilasundi keskmine paksus on 70 meetrit. Nimetatud kihtide keemilise koostise muutlikkuse uurimiseks kasutati 9 puursüdamikust võetud 392 proovi keemilise analüüsi andmeid. Proovid võeti intervalliga 0,5–2 meetrit. Põlevkivi põhielementide (MgO, P_2O_5, Al_2O_3) sisaldused varieeruvad läbilõikes suurtes piirides, näiteks CaO sisaldus muutub 3 kuni 70 massiprotsenti ja SiO_2 sisaldus 10 kuni 50 massiprotsenti, ka orgaanikasisaldus on muutlik. Lisaks on põlevkivis palju orgaanilist väävlit ja jälgelemente. Mõnede metallide (Zn, V, Cr, Ni, Mo) sisaldused läbilõikes muutuvad mitmekordselt. Keemilise koostise (18 elementi) muutlikkuse hindamiseks kasutati statistilisi meetodeid: (i) põhikomponentide analüüs, (ii) hierarhiline klasteranalüüs. Põhikomponentide analüüs näitas, et esimene põhikomponent kirjeldas 47% muutlikkust, teine 22,82%. Esimest komponenti kirjeldab orgaanikaga seotud väävli ja metallide (Cr, Cu, Ni, Zn, Mo) sisaldus ning teist positiivne korrelatsioon TiO_2, Al_2O_3, Fe_2O_3, SiO_2 ja K_2O ning negatiivne seos CaO-ga. Tulemused näitasid et, neli põhikomponenti kirjeldavad kokku ligi 89% geokeemilisest erinevusest ja nende abil on võimalik defineerida kuut erinevat põlevkiviläbilõike kivimtüüpi. Väljaeraldatud kivimtüüpide paigutus ja esinemisregulaarsus läbilõikes peegeldab lasundi sisestruktuuri. Eristunud kihid on seletatavad põhielementide/mineraalide kuhjumise intensiivsuse vaheldumisega, mis omakorda on põhjustatud märkimisväärsetest settimiskeskkonna muutustest. Põlevkivilasundi geokeemilise muutlikkuse mõistmine on oluline põlevkivi tekketingimuste selgitamise ja kaevandamise ning töötlemise seisukohalt.